Energy & Buildings 304 (2024) 113828

Contents lists available at ScienceDirect

Energy & Buildings

journal homepage: www.elsevier.com/locate/enb

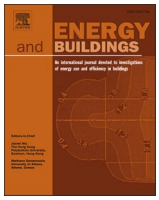

Using trickle ventilators coupled to fan extractor to achieve a suitable airflow rate in an Australian apartment: A nodal network approach connected to a CFD approach

Mikael Boulic [a,*], Pierre Bombardier [b], Zain Zaidi [c], Andrew Russell [d], David Waters [e], Andries van Heerden [a]

[a] School of Built Environment, Massey University, Albany Expressway, SH17, Auckland 0632, New Zealand
[b] Faure QEI, ATRIX Group, 20 rue Massenet, 38400 Saint Martin D'Hères, France
[c] National Association of Testing Authorities, 7 Leeds Street, Rhodes, NSW 2138, Australia
[d] Proctor Group Australia, 9 -11 Butterfield Street, Blacktown 2148, Australia
[e] APL Window Solutions, Level 2, 125 The Strand, Parnell 1151, New Zealand

ARTICLE INFO

Keywords:
Carbon dioxide
Computational Fluid Dynamic
Nodal network
Occupied apartment
Trickle ventilator
Ventilation

ABSTRACT

The level of airtightness is increasing in newly built Australian apartments. Due to the COVID-19 pandemic, restrictions have forced many people to work from home. An appropriate ventilation rate is needed to decrease virus transmission and provide occupants with a healthy environment. As occupants tend not to open windows, they need to be informed about the potential benefit of using trickle ventilators, in connection with exhaust systems, to ventilate their apartments. In 2022, a provision for lower rates of continuous ventilation (10 $L.s^{-1}$ for the bathroom exhaust system and 12 $L.s^{-1}$ for the kitchen exhaust system) was considered for inclusion in the National Construction Code of Australia. This provision was not adopted; however, this is still a valid reference for good practice. Based on this provision for continuous ventilation, our study aims to investigate the airflow velocity and the ventilation efficiency to remove the carbon dioxide (CO_2) generated across winter and summer seasons in a Melbourne apartment occupied by two adults and a child over four hours.

The study's objectives are 1) to connect two modelling approaches (Computational Fluid Dynamics and nodal networks), and 2) to investigate the potential benefits of using trickle ventilators across winter and summer seasons. The results show that wind conditions have limited effects (4% decrease in the extracted air flow rate) if the extraction network output is protected from the wind. Comparing winter and summer conditions, we found that indoor airflows differed, highly influenced by the temperature difference between outside and inside. We observed that the airflow patterns were more inclined to create "CO_2 pockets" during winter, which could increase virus transmission due to ineffective ventilation in this area. However, in winter, ventilation performed better in reducing the CO_2 concentration in the kitchen/living room area and the whole apartment than it did during summer.

1. Introduction

The National Construction Code (NCC) of Australia is performance-based [1]. The NCC requires residential buildings to have thermal resistance and ventilation of spaces where moisture can be generated. Under Section F (Health and amenity), Part F6 aims to "*ensure that building occupants have access to … fresh air, to prevent illness, injury or loss of amenity*", and the performance requirements should "*maintain adequate air quality*". NCC Table F6V1 (Verification method) gives the maximum limits for a few contaminants.

There is no published data on the airtightness of Australian apartments, but it is available for Australian detached dwellings [2,3]. Ambrose et al. (2013) investigated the airtightness level in 20 Melbourne detached dwellings [2]. The results showed a significant variation in the airtightness rate range, with the least airtight dwelling measured at 33.88 ach (at 50 Pa) and the most airtight dwelling measured at 8.07 ach (at 50 Pa) [2]. The 19.70 ach (at 50 Pa) average for the Melbourne sample was slightly higher than the 15.50 ach (at 50 Pa)

* Corresponding author.
E-mail address: m.boulic@massey.ac.nz (M. Boulic).

https://doi.org/10.1016/j.enbuild.2023.113828
Received 30 June 2023; Received in revised form 22 November 2023; Accepted 7 December 2023
Available online 15 December 2023

national sample average [3].

In New Zealand, Overton et al. (2020) investigated the airtightness in nine apartments [4]. The results showed an airtightness variation from 2.70 ach at 50 Pa (most airtight) to 8.90 ach at 50 Pa (least airtight), with an airtightness average of 5.25 ach at 50 Pa. The apartment buildings, with concrete fire partitions separating individual units, were more airtight, with an average of 3.50 ach at 50 Pa [4]. New Zealand does not have an airtightness requirement for residential buildings. This lack of regulation could explain the significant airtightness variation detected in the nine New Zealand apartment study [4].

In Australia, the NCC does not quantify an air leakage rate for new Australian buildings. It is assumed that new detached homes should achieve an airtightness rate of around 10.00 ach at 50 Pa (with currently optional verification to demonstrate permeability compliance). Since NCC 2022 should the resulting air permeability be less than or equal to 5 m^3. $hr^{-1}.m^{-2}$ at 50 Pa (broadly equivalent to 5.00 ach at 50 Pa), the building should have a mechanical ventilation system provided and following NCC Part J1V4 [1].

McNeil [5] found that New Zealand residential buildings constructed after 2000 (using construction materials and methods similar to those in Australia) were much more airtight than the ones built before 2000. The lower infiltration rate, found for more recently built structures, makes additional ventilation (natural or mechanical) necessary to dilute moisture and potential pollutants. McNeil [5] also reported a measured ventilation rate in a third of post-2000 houses very close to the estimated infiltration rates (blower door infiltration tests), indicating that the occupants seldom opened windows.

In Australia, the NCC requires that "the window, opening, door or other device have a ventilating area of not less than 5 % of the floor area" [1]. The NCC relies on occupants to open windows to reach a suitable ventilation level. This dependence on occupants for natural ventilation could only be acceptable in a draughty apartment but not in an airtight apartment. Dewsbury et al. (2016) reported that 40 % of the 2,662 surveyed Australian buildings (detached dwellings and apartments constructed after 2004) had evidence of condensation [6]. This confirms that the ventilation level was insufficient to expel the moisture generated during occupants' activities. Berneiser et al recommend that airtight residential buildings should have a low continuous ventilation unit installed to dilute the sources of pollutants unrelated to occupants' activities during unoccupied periods [7].

These findings challenge occupants' ability to open windows to reach a suitable ventilation level in post-2000 homes. NCC states that a mechanical ventilation system will be required where the 5 % of the floor area requirement for openable windows cannot be met. Other than intermittent exhaust from kitchens, bathrooms, and laundries, mechanical ventilation is seldom installed in these recently built houses, and occupants are not opening windows as the NCC assumes.

In 2022, a provision to allow for lower rates of continuous ventilation as an alternative to intermittent ventilation (10.0 $L.s^{-1}$ extraction rate for the bathroom and 12.0 $L.s^{-1}$ extraction rate for the kitchen) was proposed to the Australian Building Codes Board (ABCB). De Gids (2023) reviewed the ventilation requirements in 20 countries [8]. The review reports a significant variation between the rate of 8.3 $L.s^{-1}$ and 42.0 $L.s^{-1}$, with an average continuous ventilation rate of 19.0 $L.s^{-1}$ for the kitchen and a significant variation between the rate of 7.0 $L.s^{-1}$ and 22.0 $L.s^{-1}$ with an average continuous ventilation rate of 14.0 $L.s^{-1}$ for the bathroom. This proposed requirement rate (10.0 $L.s^{-1}$ in the bathroom and 12.0 $L.s^{-1}$ for the kitchen) will rank Australia at the 15th lowest position (same position as New Zealand) out of the 20 countries surveyed for ventilation rate [8]. The ABCB did not adopt this ventilation compliance pathway. Finally, NCC 2022 (F8D4 Exhaust Systems) provisions for bathrooms did not change from NCC 2019, except that the bathroom exhaust system is interlocked with the light switch and must operate for 10 min after the light switch is turned off. For kitchen ventilation, NCC 2022 provisions did not change from NCC 2019, except ABCB expanded ventilation requirements to kitchen range hoods, which need to be discharged outdoors and not to the roof space [1].

Despite the ABCB not adopting this ventilation compliance pathway, this is still a valid reference for good practice. This was the rationale for using this proposition in our case study.

During the COVID-19 pandemic, restrictions have forced many people to work from home. Under these circumstances, it is crucial to ensure that occupants are able to experience a well-ventilated environment when spending more time at home. SARS-CoV-2 is transmitted via droplets and contact with surfaces. It is well established that a poorly ventilated dwelling will favour the transmission of the virus, even if social distancing is respected [9–11]. To reduce SARS-CoV-2 transmission in the indoor environment, Morawska et al recommend effective ventilation, enhanced with air filtration and disinfection in addition to personal protective equipment and social distancing [12]. Air recirculation should be avoided.

In the case where an occupant is infected, the home, or part of the home, could be used as a quarantine space. In the roadmap to "*ensure good indoor ventilation in the context of COVID-19*", WHO recommends a minimum of 10 $L.s^{-1}$ per person within the isolation area, and the isolation area should ideally be separated from the rest of the house [13]. In addition, if this strategy cannot be followed, the occupants should consider using a stand-alone air cleaner MERV 14. A higher flow rate (12.5 L. s^{-1} per person) is recommended in Spain to ventilate the isolation area effectively and reduce virus transmission [11]. Picard et al investigated the transmission of SARS-CoV-2 from the isolation room (infected person in a bedroom) to the other household members located in the other rooms of a single dwelling. They found that the risk of contamination could be reduced by 80 % if all household members wore a mask, the isolation room door was closed, the undercut was blocked at 90 %, and the isolation room window was open during the day [14]. Guyot et al investigated the virus transmission from an infected apartment to neighbouring apartments. The results showed that keeping the infected apartment's internal doors open increased the contamination rate in the same apartment but decreased the exposure to viruses for occupants of neighbouring apartments [15]. Guyot et al found that the apartment corridor could be used as a buffer zone to reduce contamination (distancing effect). Research strongly supports the use of masks, social distancing, and effective ventilation as protective strategies against virus contamination. However, more research is needed to understand the dynamics of airflow-carrying viruses. Our research will contribute to filling this gap.

Berneiser et al reported from a German survey that outside noise was a critical factor in windows not being opened for ventilation [7]. A Melbourne, Australia survey supports these results, reporting that two-thirds of respondents were disturbed during the night by noise when opening windows, and 43 % did not open windows for ventilation during the day due to excessive noise [16]. The same study also reported thermal discomfort during the summer (overheating) connected to this reduced natural ventilation. A Spanish survey on natural ventilation, undertaken during the first wave of the COVID-19 pandemic, reported that elderly and young people tend to open windows less than middle-aged people [17]. Using a trickle ventilator (equipped with acoustic treatment) could be an effective ventilation strategy when occupants are not opening windows. Using trickle ventilators could assist in effectively ventilating their indoor environment during pandemics. However, the trickle ventilators are useful only in low-polluted outdoor areas. Xu et al monitored the indoor environment in a three-bedroom apartment in Nanjing, China. The authors concluded that due to an outdoor level of $PM_{2.5}$ (particulate matter of 2.5 μm or less in diameter) above the WHO 70 $\mu g.m^{-3}$ in winter, it is recommended to use a fresh air system with an air purifier rather than directly outside air for ventilation [18].

Our research proposes to connect two modelling approaches (Computational Fluid Dynamics and nodal networks) to investigate the use of trickle ventilators connected to extractor fans as potential ventilation solutions in one Australian apartment.

Computational Fluid Dynamics (CFD) modelling is a well-accepted

approach to designing and evaluating ventilation strategies in the built environment [19]. The CFD software will generate air velocity and temperature values for each defined cell in the mesh [20]. Any update of the input values will require the software to reprocess the whole model. This extensive dataset processing involves significant computational power, a weakness of the CFD approach. To reduce the computational need and speed up the process, some authors proposed combining the CFD approach with a nodal network approach [21]. In the nodal network approach, the space would be defined as "a number of linked nodes" [22] where the temperature values and the air velocity values could be aggregated into a single bulk of temperature value and a single bulk of air velocity value. When used jointly, these two approaches complement each other. The nodal network approach will assist in defining the CFD boundary conditions and dramatically decrease the need for computational power [23].

Our approach is described as a one-way coupling technique (also called partial coupling) of a nodal network to CFD modelling [24]. This one-way coupling approach dramatically reduces the computational need and fastens the process. The nodal network approach selects a few interesting cases, which will be investigated later using the CFD approach. For example, the nodal network approach could assist in choosing a "normal operating condition" and a "degraded operating condition". This degraded condition impacts the boundary conditions (fan extractor flow rate and, subsequently, the air change rate in the apartment). A partial coupling is recommended as it significantly reduces the involved computational power, a weakness of the CFD approach. A review from Kato et al supports this partial coupling approach; the authors do not recommend a full coupling (two-way input of pressure and temperature data) that will dramatically increase the computational need and slow down the calculation process [23].

Our study aims to investigate the airflow velocity and the ventilation efficiency to remove the carbon dioxide (CO_2) generated across winter and summer seasons. Bhagat et al observed that CO_2 flowed similarly to virus particles in the breathing zone, so CO_2 distribution could approximate the virus particle distribution in the apartment [25].

2. Methodology

2.1. Presentation of the case study

The case study is a 90 m^2 two-bedroom apartment in Melbourne, Australia.

Fig. 1 shows the studied 21st-floor apartment in the 45-story building.

The 90 m^2 apartment comprises seven rooms (Fig. 1, right): a primary bedroom with ensuite, a kitchen and living area, an office, a child bedroom, a second bathroom and a laundry. According to Bruce Henderson Architects (2018), in New South Wales (Sydney), "*The new standard sets the size of a two-bed unit at 91 m^{2}*" [26]. However, in Victoria (Melbourne), "*The average size of the two-bedroom units shrank to 59 m^2 from 62 m^2*." The average size of an apartment tends to be smaller in Melbourne than in Sydney [27]. Our 90 m^2 case study apartment is larger than Melbourne's apartment average size and follows Sydney's apartment average size. However, our Melbourne case study was taken from an actual floor plan from a developer.

The air enters the apartment via five trickle ventilators and is extracted via three extraction grilles connected to a fan extractor.

Fig. 2 shows the location of the five trickle ventilators installed on the North-facing windows (T1: primary bedroom, T2 and T3: living/kitchen area, T4: office and T5: child bedroom). The three extraction grilles are in the second bathroom (E1, with a continuous flow rate of 10 $L.s^{-1}$), in the kitchen (E2, with a continuous flow rate of 12 $L.s^{-1}$) and the primary ensuite (E3, with a continuous flow rate of 10 $L.s^{-1}$) respectively. Under a continuous extraction regime, the air flowing through the trickle ventilators could be influenced by the dynamic pressure applied due to the wind force on the external building surface.

We removed the laundry volume (red cross in Fig. 2) because it is treated as a closed room without any air extraction (like a cupboard). A clothes drier would either be ducted directly to the exterior or of heat pump or condenser type. Removing the laundry volume could reduce the time for CFD calculation and will not impact the final results (no loss of information on occupants' exposure to potential contaminants).

Fig. 3 shows the profile of the trickle ventilator used in the CFD simulation [28].

All five trickle ventilators are the same size: 70 cm by 5.5 cm, with an effective open area of 32.2 cm^2. The trickle ventilator, adapted to the window frame dimensions, incorporates a passive wind dampener to manage water ingress and draughts associated with high wind gusts. This model is representative of the horizontal-flow-type of trickle ventilator and includes a shape memory alloy adapting the opening to external temperature (fully open above 18 °C and one-third open under 12 °C external temperature).

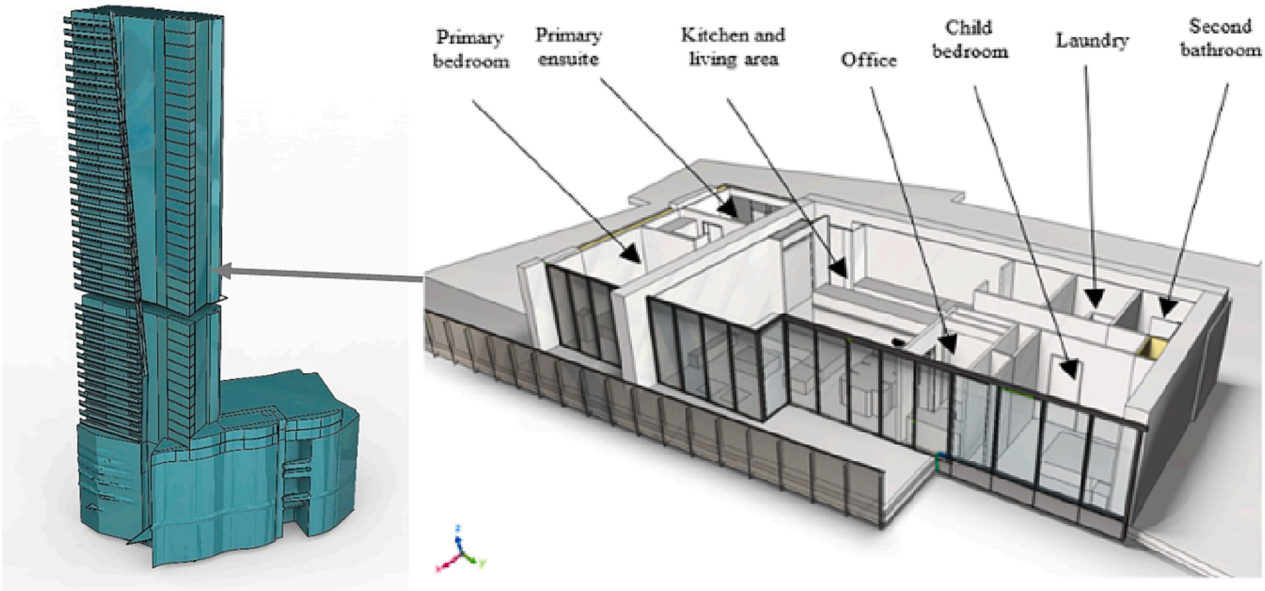

Fig. 1. The 45-storey building with the 21st-floor apartment location (left) and the apartment's composition (right).

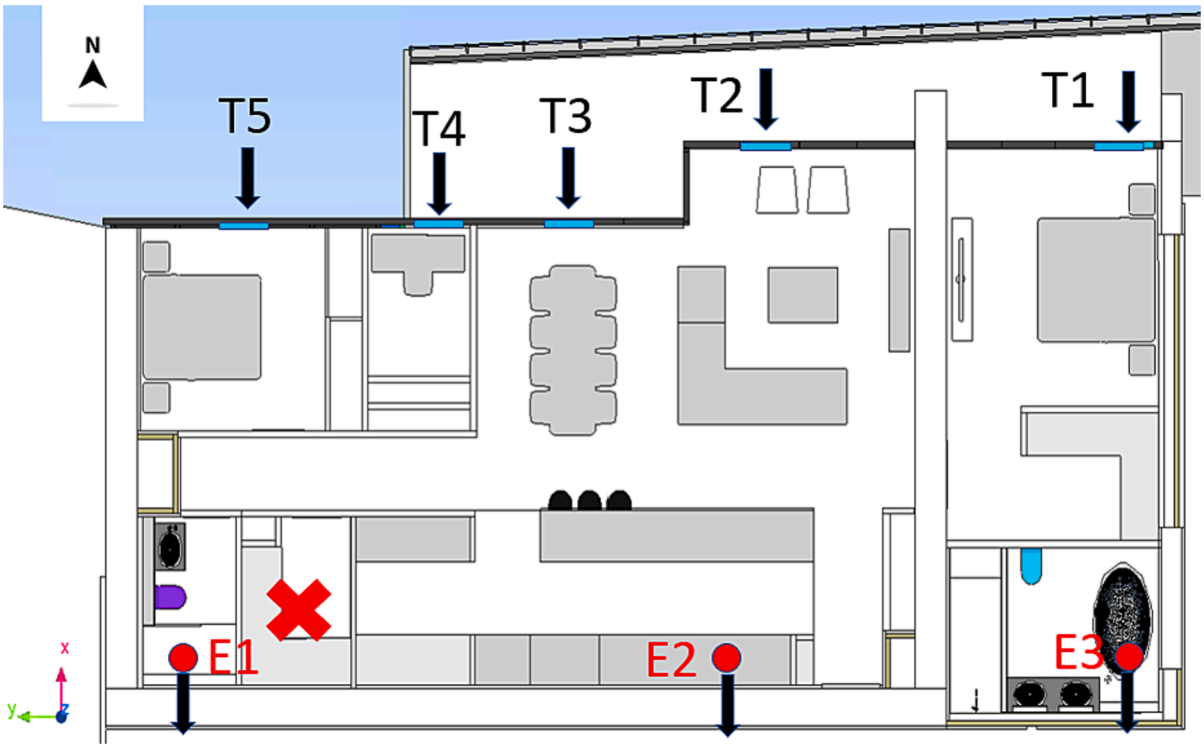

Fig. 2. The two-bedroom apartment plan with cross-ventilation features. Three fan extraction grilles: E1-E3 (on the South side) and five trickle ventilators T1-T5 (on the North-facing window frames). The laundry volume (red cross) was removed from CFD simulations. (For interpretation of the references to colour in this figure legend, the reader is referred to the web version of this article.)

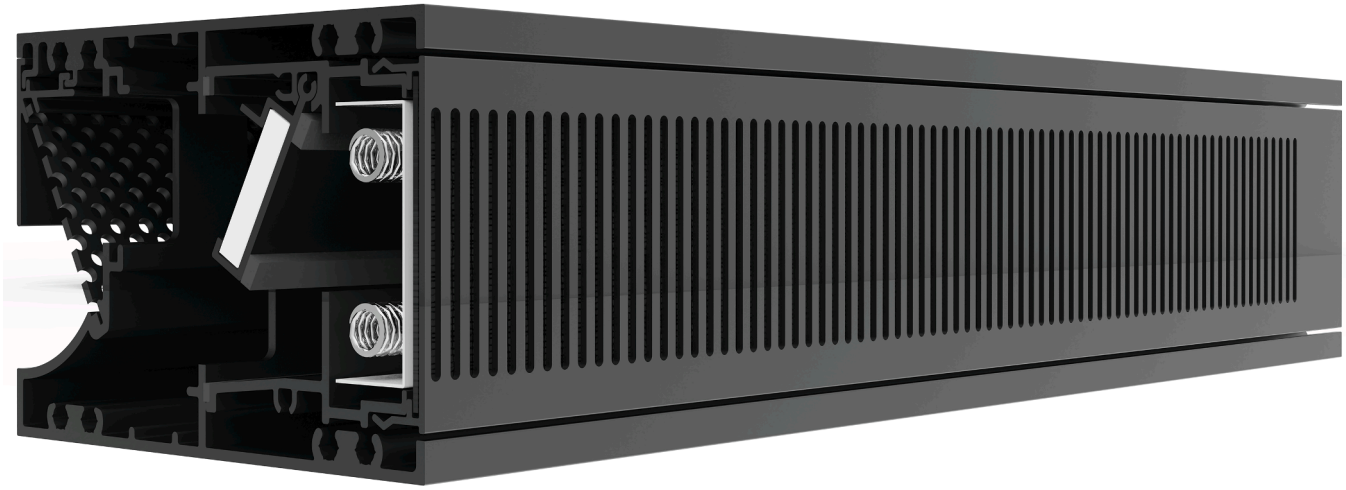

Fig. 3. 3D model of one trickle ventilator (source: APL Window Solutions, model Ventient SCW-SH700).

A total air intake of 32.0 L.s^{-1} (10.0 L.s^{-1}: primary bathroom flow rate, 12.0 L.s^{-1}: kitchen flow rate and 10.0 L.s^{-1}: second bathroom flow rate) was used.

As there are five trickle ventilators, we assumed that each ventilator would have a mean airflow of 6.4 L.s^{-1} (equivalent to 23.04 m^3.h^{-1}).

This 32.0 L.s^{-1} total flow rate follows the NCC 2022 draft provision for continuous ventilation, which is twice the NCC current performance requirement rate (15 L.s^{-1}) for a 90 m^2 two-bedroom apartment (with an air permeability rate of not more than 5 m^3. hr $^{-1}$. m^{-2} at 50 Pa) over four hours (NCC Part J1V4) [1]. In the context of COVID-19, this flow rate of 32.0 L.s^{-1} follows the WHO recommendations of 10.0 L.s^{-1} per person [13] within the isolation area (assuming three persons, which was our selected case study).

2.2. Conceptual framework coupling the nodal network and the CFD models

Fig. 4 shows the conceptual framework of our study. A nodal network and two CFD models are connected.

The first step (CFD building external surface) defines the wind velocity range on the input face of the trickle ventilators (airflow entering the apartment through the five trickle ventilators). The wind boundary conditions (average wind velocity) are defined for the three dominant wind directions (North, South and Southwest) as reported in Section 2.3.

The second step (nodal network) simulates the behaviour of the three extractor grilles (under normal and degraded operating conditions).

The nodal network approach considers the airflow through the fan

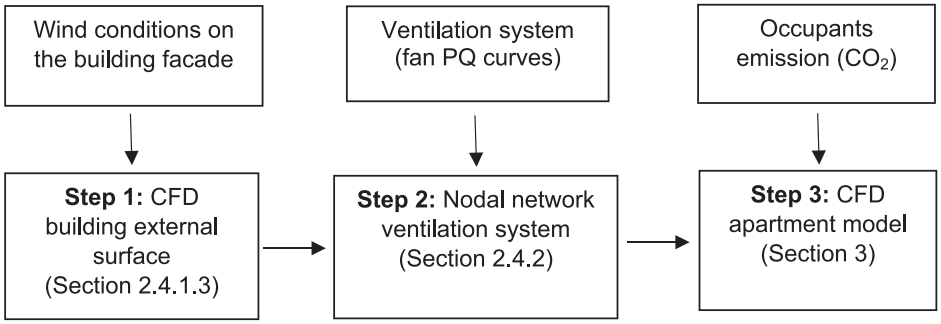

Fig. 4. Conceptual framework connecting a nodal model and two CFD models.

extractor (using the static pressure/air volume - PQ curves and the outcomes from the CFD building's external surface. The nodal network is manually linked to the CFD apartment model to define the boundary conditions to apply (correction on airflow rates due to external wind conditions).

In the CFD apartment model, we investigate both the airflow behaviour and the ventilation efficiency when using CO_2 generated by occupants as a tracer gas (a proxy for the ventilation rate). Bhagat et al observed that CO_2 flowed similarly to virus particles in the breathing zone, so CO_2 distribution could approximate the virus particle distribution in the apartment [25]. We followed the 2023 NCC Indoor Air Quality Verification Methods Handbook for the recommended 1000 ppm CO_2 level for adequate ventilation rate [29]. This Handbook states, "*There is growing evidence that carbon dioxide levels above 1000 ppm can result in reduced levels of concentration in humans and reduced work performance and productivity levels. However, elevated carbon dioxide concentrations also indicate inadequate ventilation that tends to increase the concentrations of all contaminants with indoor sources*" (page 26) [29].

2.3. Wind boundary conditions

This apartment is in Melbourne, Australia. We implemented the wind data in our CFD building's external surface. There are four main weather stations in the Melbourne metropolitan area (Melbourne, and Essendon airports, Fawkner Beacon in Port Phillip Bay, and Moorabbin Airport). Holmes (2021) adjusted the data from the four weather stations for terrain conditions and height and found similar distributions for all four stations when investigating the parameters from all directions (Weibull distribution method) [30]. Our wind data are extracted from Melbourne Essendon Field Airport Weather Station [31].

Fig. 5 shows the prevailing wind direction according to the months. The wind direction was measured at 10 m high from 1980 to 2016.

Fig. 5 shows that the wind predominates from the North during the April - September period, with a peak during the winter (June - August). The wind prevails from the West during September and October. The wind predominates from the South from October to April, peaking around summer (December-February). We implemented these three prevailing wind directions (North, South and Southwest) in the CFD building external surface model. The yearly average wind velocity was estimated at 4.5 $m.s^{-1}$ for the three wind directions [31].

2.4. Modelling

2.4.1. CFD modelling approach

We connect two CFD models and a nodal network in our proposed methodology. The first CFD model targets the external building façade (Section 2.4.1.3). A nodal network approach (Section 2.4.2) considers the airflow through the fan extractor (using the static pressure/air volume - PQ curves) and the outcomes from the CFD building external surface model.

The CFD building's external surface is defined as a steady-state model. In contrast, the CFD apartment model is transient, with a simulation over four hours.

2.4.1.1. The CFD equations. The general equations used in these CFD simulations can be found in reference [20]. These equations are based on the mass, energy, and momentum conservation laws. The CFD modelling was undertaken using scSTREAM, a commercial CFD software (Cradle CFD part of Hexagon Manufacturing Intelligence, Hexagon AB Group, Sweden).

The CFD simulation employs turbulence models to simulate fluid motion and the appearance of eddies. These turbulence models are

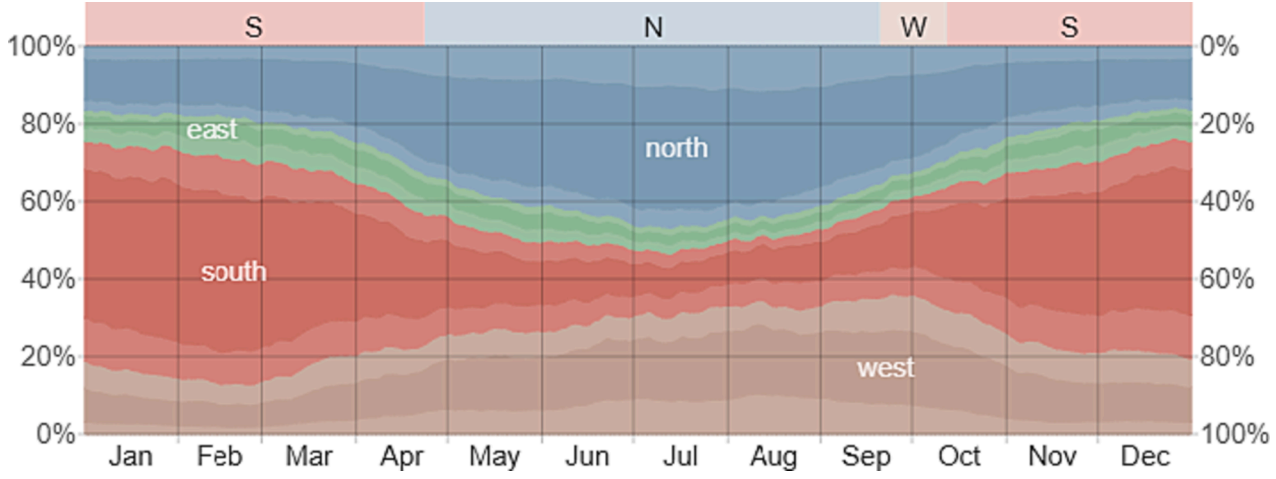

Fig. 5. Prevailing wind direction per month in Melbourne, Australia (WeatherSpark.com).

specific to different situations, and a significant research effort has been dedicated to their development [32]. In ventilation studies, air turbulence is usually described using the Reynolds-Averaged-Navier-Stokes (RANS) equations [33,34]. Derived from the RANS equations, several models have been developed, like the ReNormalization Group (RNG) K-epsilon turbulence model, which we selected to study the wind impact because it is well-suited for the prediction of flows around buildings [35]. The AKN model, a Linear Low Reynolds (LLR) model [36], is selected for indoor ventilation simulations as it improves the prediction accuracy in the near-wall region (low Reynolds number) where the turbulence arises [37]. These models are commonly used for airflow simulation in the built environment [38].

2.4.1.2. Computational grid and convergence. scSTREAM has a finite volume discretisation scheme. The computational grid is a structured hexahedral mesh defined following the CFD good practices [39]. A sensitivity analysis was run after refining the volumes where considerable pressure or velocity gradients were expected, and then the grid convergence was obtained. The solver convergence was assessed by meeting residual error convergence criteria (10^{-6} level) and stability for monitoring points (pressure velocity and CO_2). The final mesh includes 6 to 8 million nodes for the models described here.

2.4.1.3. CFD building external surface model (Step 1). Fig. 6 shows a large-scale model (with the space above the building of 735 m, the area on each side of 339 m, the length in front of the structure of 735 m and the space behind the building of 2,205 m, for a total of nine million nodes). The wind boundary conditions were implemented, and the output defines the wind velocity range on the input face of the trickle ventilators (airflow entering the apartment through the ventilators). This CFD building external surface model was scaled following the code of best practices for the CFD simulation of flows in the urban environment [40]. We also followed the scSTREAM Cradle instruction manual to define the boundary conditions applied to the computational domain boundaries [37,41].

Fig. 6 shows the wind velocity on the building's external surface when the wind comes from the North (prevailing during the winter season).

Fig. 7 shows the wind pressure on the building's external surfaces when the wind comes from the South (prevailing during the summer season). A pressure of −7.9 Pa was estimated on the North-facing façade (input of the trickle ventilators).

Table 1 shows the pressure results on the North-facing external surface of the building according to the direction of the wind. We used a value of 4.5 $m.s^{-1}$, the yearly average wind velocity, measured at 10 m high [31].

Table 1 shows a negative pressure of −7.9 Pa, which will be applied on the North-located trickle ventilator during the dominant South wind direction (summer season). In reverse, a positive pressure around 19.0 Pa will be applied on the North-located trickle ventilator during the prevailing North wind direction (winter season). These pressure results were input into the nodal network modelling.

2.4.2. The nodal network approach (Step 2)

We used SYLVIA, a nodal network software (developed by the Institute for Radiological Protection and Nuclear Safety – IRSN, France). This nodal network software has been validated for mechanical ventilation modelling, considering the wind effect under a steady state regime [42,43]. One of the SYLVIA software applications is the study of the behaviour of a ventilation network in normal or accidental operating conditions [44–46]. The use of the nodal network approach assists in predicting the impact of wind distribution on the mechanical ventilation system efficiency. As not all conditions could be investigated using a CFD approach, the nodal network software will assist in defining the degraded conditions, like the overpressure effect due to high wind or the impact of the internal doors opening vs. closing in the apartment. A high number of variables (environmental constraints like wind pressure, occupants' behaviour like door opening/closing) and a high number of values available for each variable will create many potential scenarios. The nodal network approach informs on the CFD models' possible boundary condition values input. We focus on normal operating conditions and degraded fan extractor operating conditions (like shutting down the fan and installing a non-protected extraction façade outlet). This degraded condition impacts the fan extractor flow rate and, subsequently, the air change rate in the apartment. This nodal network approach assists in dramatically reducing the need for computational power. The computer power needed to conduct nodal network simulations is much lower than required for the CFD modelling, and the fastest results are obtained from nodal network calculations.

2.4.2.1. Nodal network physical components and definitions. The ventilation network is divided into a series of nodes (zones of uniform pressure), which connect to junctions (branches) and components (fan, door).

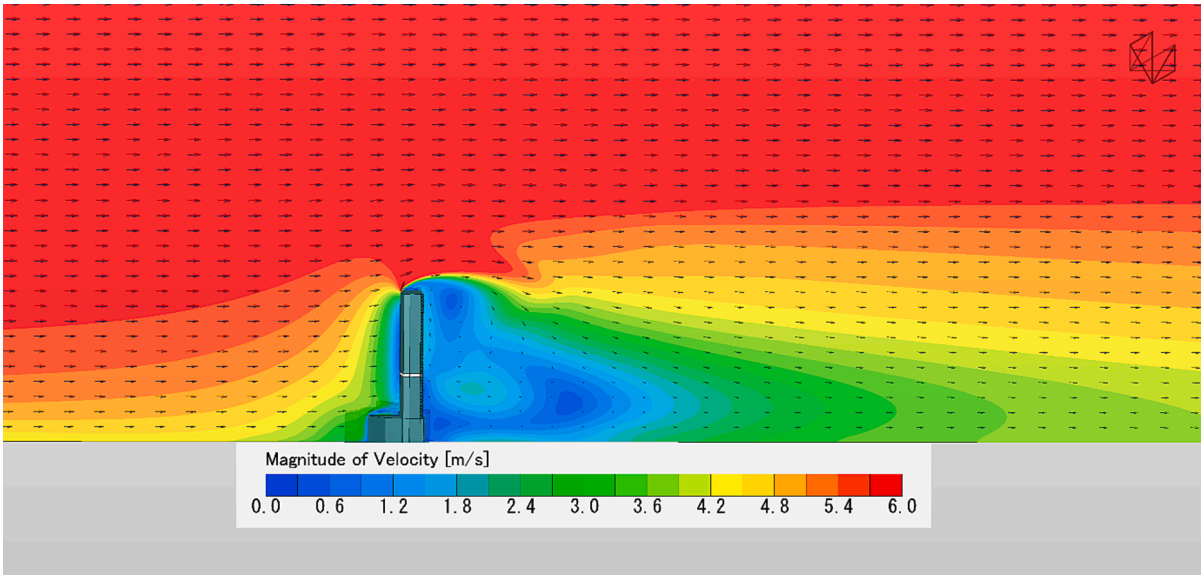

Fig. 6. CFD external surface showing the wind velocity (m.s-1) with a North wind.

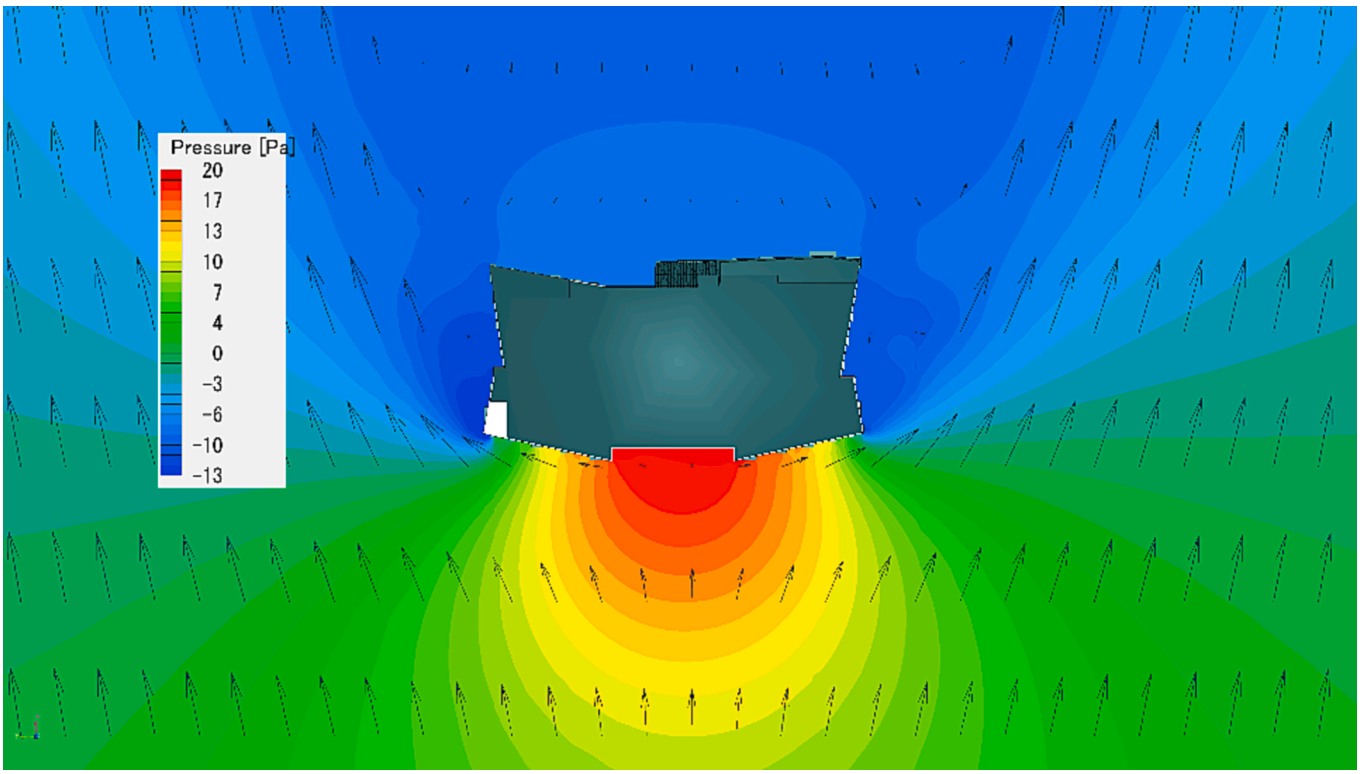

Fig. 7. CFD external surface showing the wind pressure (Pa) with a South wind.

Table 1
Resulting pressure on the external surface due to wind (direction and velocity).

The three prevailing wind directions	Wind velocity ($m.s^{-1}$)	Pressure on the North-facing external surface (Pa)
North *(winter season)*	4.5	19.0
South (*summer season*)	4.5	−7.9
South–West (*September/ October, spring season*)	4.5	−7.0

When we built our ventilation network, we used six variables (symbols), which are as follows:

- The node symbol (.) describes a local junction in a static calculation,
- The "rake shape" symbol ( ) defines the boundary condition, for example, the atmospheric pressure,
- The "spring shape" symbol ( ) symbolises the quadratic resistance that could represent a ducting or a trickle vent pressure drop,
- The "register" symbol ( ) defines the aeraulic resistance, which is a function of the damper opening angle,
- The "door opening" symbol ( ) represents a valve or a door with two statuses (either open or closed),
- The "diode-like" symbol ( ) represents a non-controlled fan, which is defined by flow rate (pressure dependent).

2.4.2.2. Nodal network architecture. Following the ventilation nodal network build-up, the system is filled with pressure values, flow values, fan curves, and regulation parameters as instructed in the user's guidelines [46]. Before calculating the different scenarios, the resistances are calculated and fixed, and the flow balance is tested. The last step consists of simulating the extractor fan operating conditions under two regimes: the regular regime (experienced most of the time) and the degraded regime (experienced in special conditions). The degraded condition result informs on the extractor fan operating under significant constraint.

Fig. 8 shows the nodal network built for the studied Melbourne apartment.

2.4.2.3. Nodal network boundary conditions. Both the input and the output of the network are the ambient air. The air enters the apartment through the five trickle ventilators and is extracted through the inline fan (equivalent to E1 + E2 + E3 = 32.0 $L.s^{-1}$). In the nodal network, the three exhaust fans are represented by one inline fan ("diode-like" symbol) because each exhaust fan is connected to a register that defines each fan's aeraulic resistance. The air from the child's room and the office will pass the door undercuts (2 cm) and be mixed in the corridor/living room open space before extraction through mainly the 2nd bathroom and kitchen exhaust units. The input pressure comes from the CFD building's external surface, as shown below in Table 2. The air extraction is controlled by the extractor fan Q (air volume)/P (static pressure) curve and the outside pressure on the fan.

In the studied apartment, five doors could be opened or closed. This door system could consist of $5^2 = 25$ conditions. Our reported simulations only considered two cases: during the day (all doors opened) and at night (bedroom doors closed).

Table 2 shows the resulting outputs according to the wind direction, wind velocity, door status, and pressure on the vents or extraction fan.

The nodal network estimates the airflow ($m^3.h^{-1}$) at each component level (trickle ventilators, primary ensuite grille, second bathroom grille, kitchen grille and internal transfers) and the total airflow. Only the total airflow is reported here.

Table 2 shows that under northerly wind (prevailing in the winter season), the airflow increased by 9 % (compared to a reference case with no wind). In reverse, under southerly wind (prevailing in the summer season) or prevailing southwest wind, the airflow is decreased by 4 %. This southerly wind puts pressure on the trickle vents, which could be considered a degraded regime. In a specific case of a non-protected extraction fan outlet (18 Pa), the airflow could be reduced by another 9 % to a total reduction of 13 % (another case of the degraded regime),

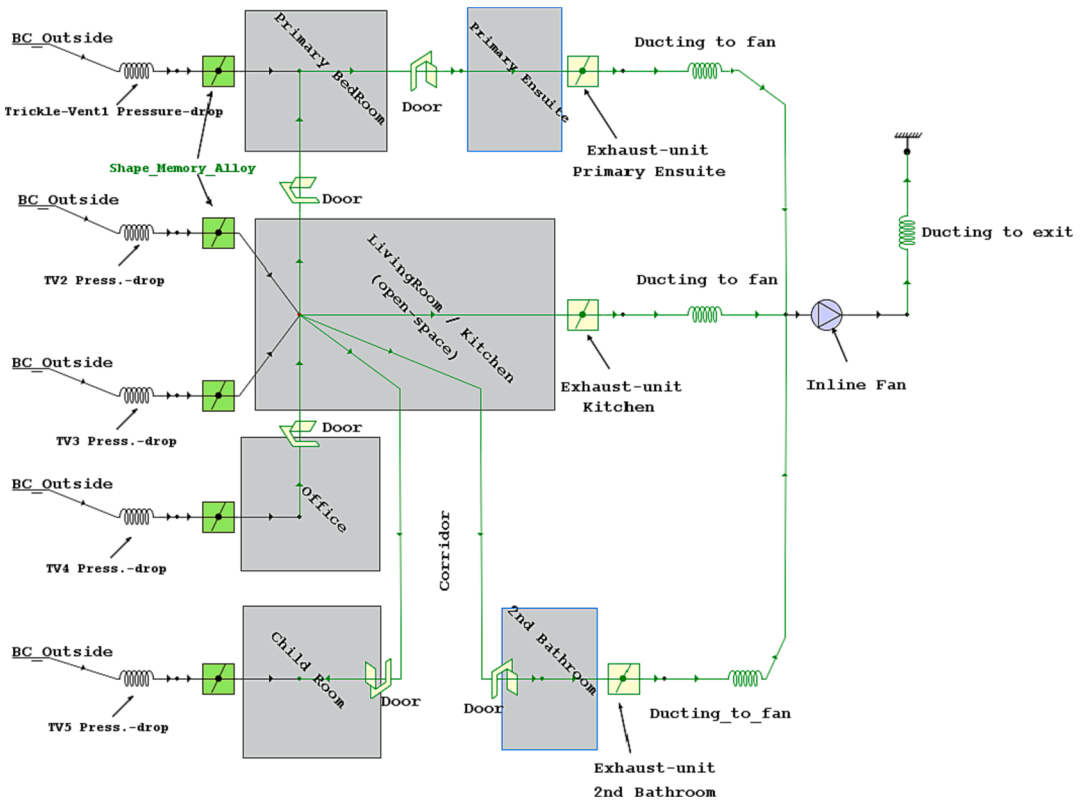

Fig. 8. A nodal network of the studied apartment (BC: building external surface conditions, TV: trickle vent).

Table 2
Inputs and outputs of the nodal network modelling according to input conditions.

Inputs to the nodal network					Outputs from the nodal network	
Wind direction	Wind velocity ($m.s^{-1}$)	Door status	Outside pressure on trickle vents - air input (Pa)	Outside pressure on extraction fan - air output (Pa)	Total airflow ($m^3.h^{-1}$)	Airflow variation (%)
Reference	0	All doors open	0	0	115.0	0
North	4.5	All doors open	19.0	0	124.8	9
South	4.5	All door open	−7.9	0	110.6	−4
South	4.5	All door open	−7.9	18.0	100.0	−13
South	4.5	Bedrooms doors closed	−7.9	0	110.6	−4
South -West	4.5	All doors open	−7.0	0	111.2	−3
South -West	4.5	Bedrooms doors closed	−7.0	0	111.2	−3

equivalent to a decrease of 15 $m^3.h^{-1}$. In reverse, the nodal network results showed that opening or closing the bedroom doors did not impact the total airflow.

The nodal network results will be manually linked to the CFD apartment modelling (partial coupling).

In the final CFD apartment modelling, we will use the CO_2 generated by the occupants over four hours as a tracer gas. We will investigate the airflow path and the ventilation efficiency to remove the CO_2 generated in winter and summer and at two heights (300 mm and 1500 mm - breathing zone) from the floor.

2.4.3. Occupants generated carbon dioxide (CO_2)

We assumed that this two-bedroom apartment is occupied by two adults (one male, 40 years old and one female, 40 years old) and one child (10 years old). The occupants stay in this apartment and undertake light effort tasks (MET 1.5) for four hours. The rationale for selecting four hours and light tasks is connected to potential COVID-19 restrictions that pushed many people to work from home or stay in their apartments for extended periods.

Our study investigates the airflow path and the ventilation efficiency to remove the CO_2 generated across winter and summer seasons.

Fig. 9 shows the developer 3D model imported to the CFD program to create the apartment model.

The two adults are in the kitchen/living area, and the child is in the office. Fig. 9 shows the locations with a good likeliness of presence (where people are likely to stand or sit in the living room and the office: the yellow volumes). Table 3 shows the CO_2 generation rate ($L.s^{-1}$) for each of the three occupants during sitting tasks/light activity (MET 1.5). We assumed that the CO_2 sources are generated at a constant rate over four hours.

As explained in our conceptual framework, the results from the nodal network and the generated CO_2 concentration will input the CFD apartment model. The results of the CFD apartment model (final model) are reported in the Results Section.

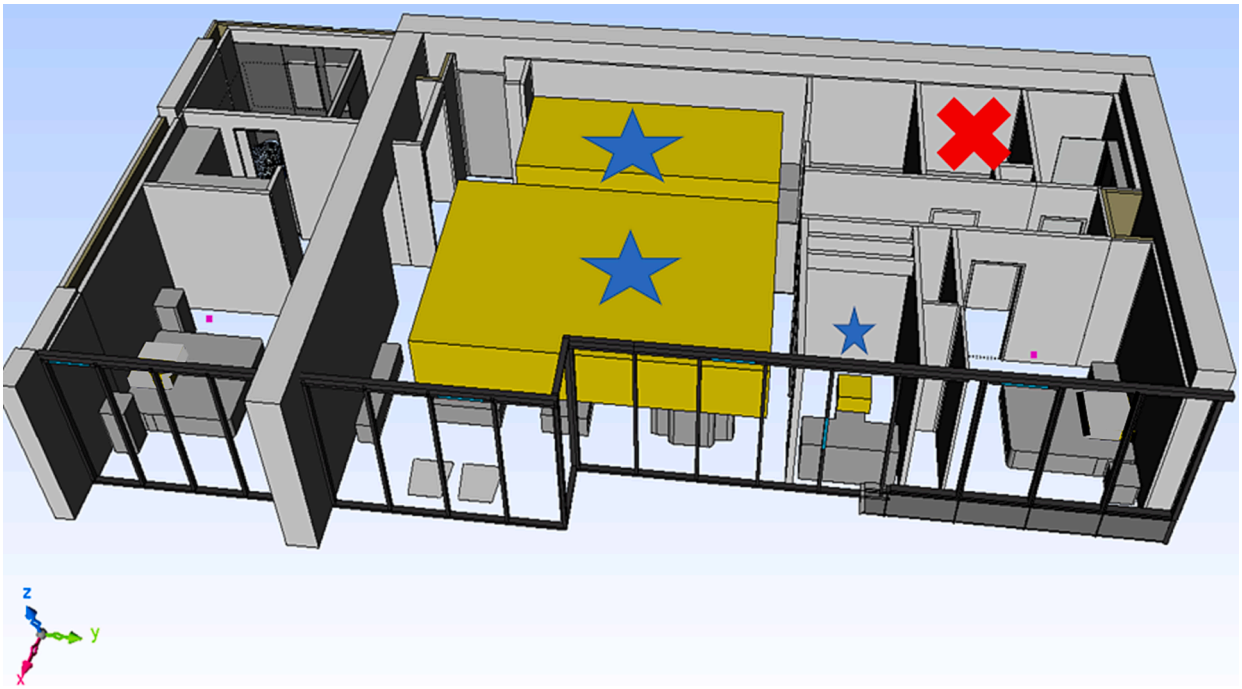

Fig. 9. Location of the three occupants (three blue stars: two adults in the kitchen/living area and one child in the office area) and places with a good likeliness of CO_2 generation (yellow volumes). (For interpretation of the references to colour in this figure legend, the reader is referred to the web version of this article).

Table 3
Carbon dioxide generation rate ($L.s^{-1}$) at MET 1.5: sitting tasks, light effort [47].

Occupants in the apartment	Location of the source	CO_2 generation rate at MET1.5 ($L.s^{-1}$)
One male (40 years old)	Living room	0.0058
One female (40 years old)	Living room	0.0045
One child (10 years old)	Office	0.0037

3. Results and discussion

The results section focuses on the CFD apartment model, where we will investigate both the airflow behaviour and the ventilation efficiency in the apartment when using carbon dioxide (CO_2) as a tracer gas. This CFD apartment model will use results from the nodal network and the CO_2 generated by the occupants for four hours. Fig. 10 is a close-up of the conceptual framework (presented in Fig. 4).

In the first part of the results, we will compare the airflow path and the ventilation efficiency between a winter case study (prevailing northerlies at an input temperature of 12 °C) and a summer case study (prevailing southerlies at an input temperature of 20 °C). This comparison will be undertaken at two heights (0.30 m from the floor and 1.50 m from the floor, representing the breathing zone). The second part of the results will look at the impact of the season on the CO_2 concentration in the breathing zone (1.5 m from the floor).

3.1. Air flow path and ventilation efficiency across summer and winter seasons

Fig. 11 and Fig. 12 show the velocity of the airflow path from the air entrance (five trickle vents) to the air extraction (three grilles). Fig. 11 (left) displays the airflow path during the summer (prevailing South wind with an ambient temperature of 20 °C) at the height of 0.30 m from the floor. Fig. 11 (right) displays the airflow path during the winter (prevailing North wind with an ambient temperature of 12 °C) at the height of 0.30 m from the floor.

The summer airflow profiles through the trickle ventilators for the air at 20 °C (same temperature as room temperature) follow a 45° angle. In contrast, the winter airflow profiles through the trickle ventilators for the air at 12 °C (intake temperature is 8 °C cooler than the 20 °C room temperature) quickly fall to the floor. An 8 °C difference for the winter case study creates a higher air flow velocity at 0.30 m from the floor (winter case study airflow: between 0.035 $m.s^{-1}$ and 0.050 $m.s^{-1}$ vs. summer case study airflow: around 0.010 $m.s^{-1}$). This 12 °C airflow could create discomfort for people sitting close to the windows.

Fig. 12 (left) displays the airflow path during the summer case study (prevailing South wind with an ambient temperature of 20 °C) at the

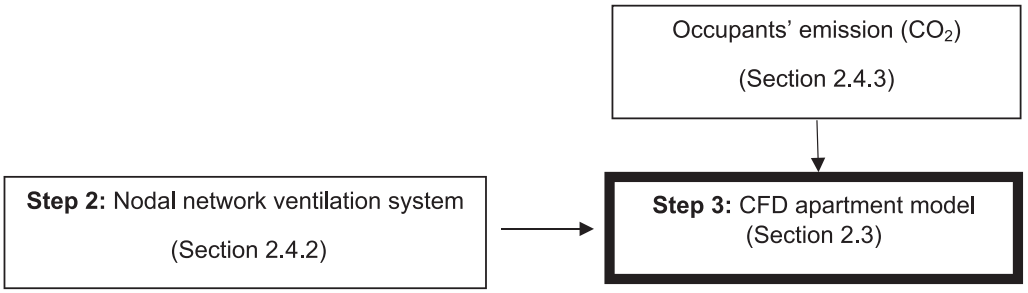

Fig. 10. Conceptual framework defining the CFD apartment model.

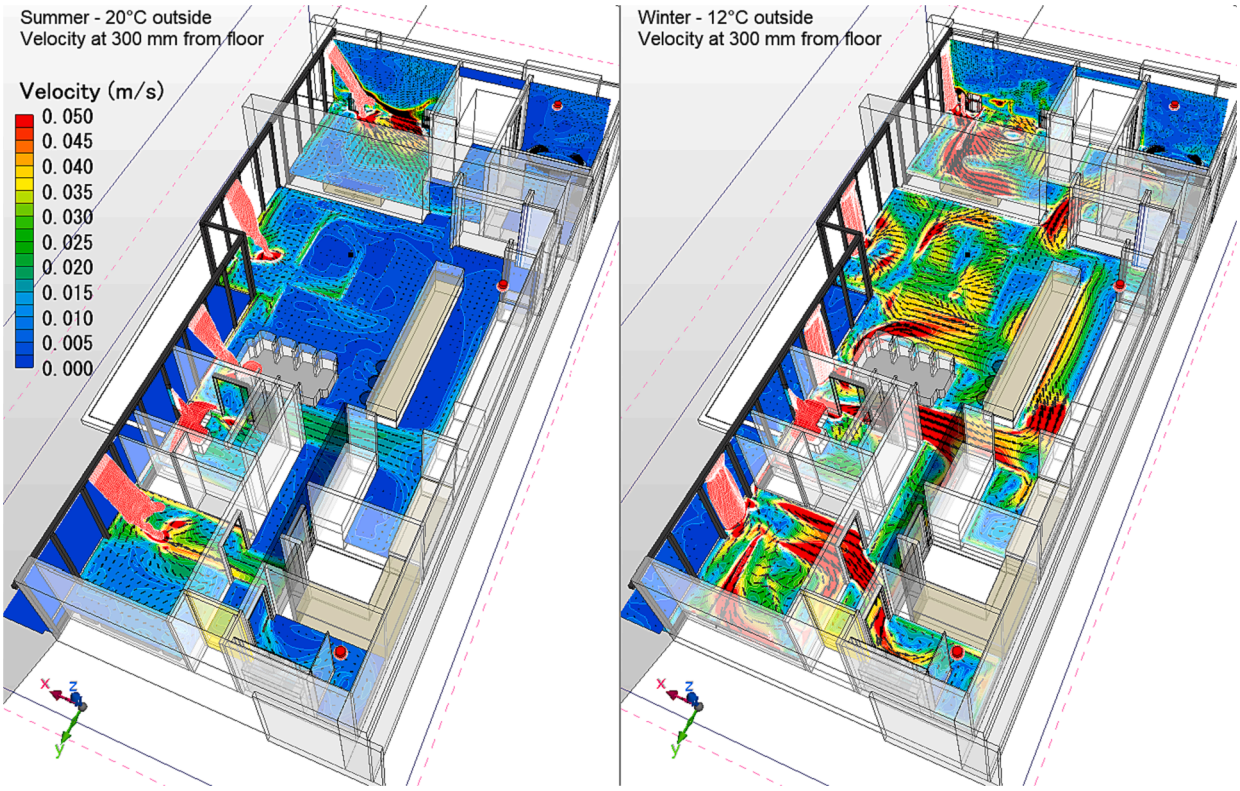

Fig. 11. Airflow paths during summer (left) and winter (right) at the height of 0.30 m from the floor.

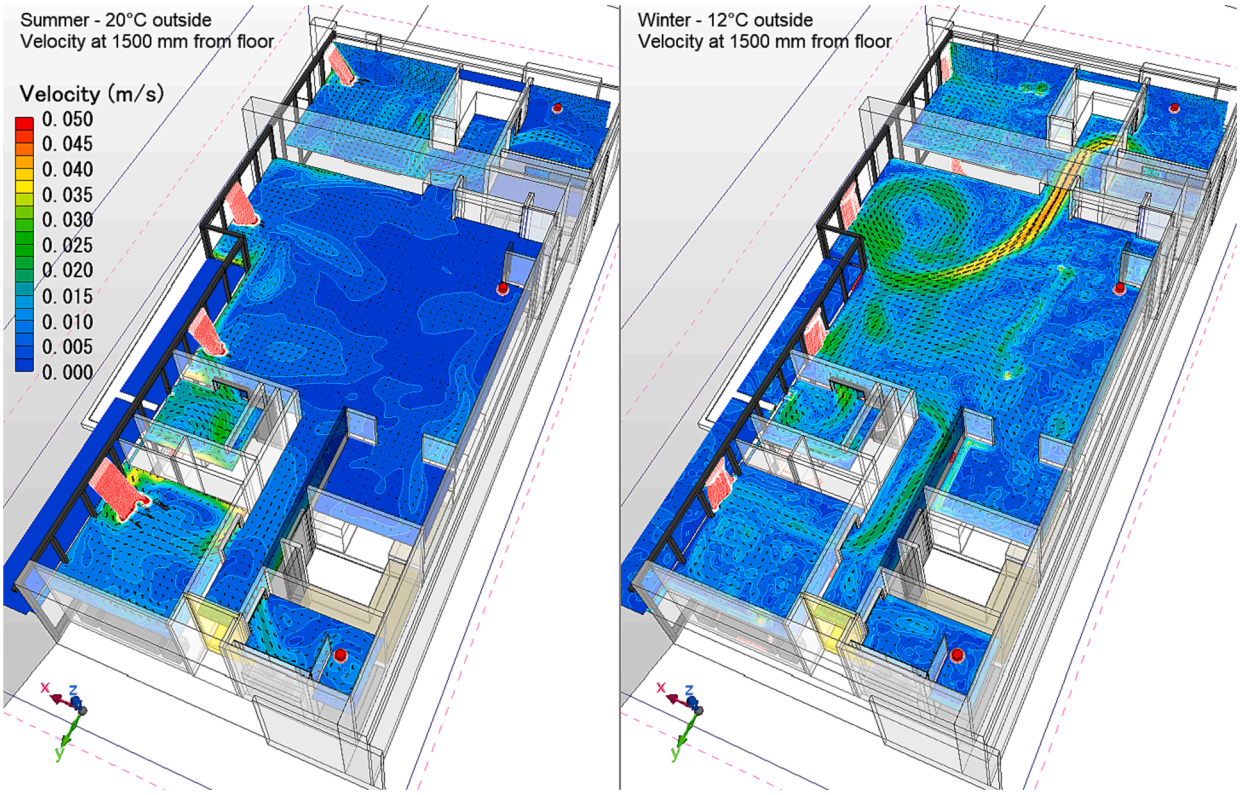

Fig. 12. Airflow paths during summer (left) and winter (right) at the height of 1.50 m from the floor.

height of 1.50 m from the floor. Fig. 12 (right) displays the airflow path during the winter case study (prevailing North wind with an ambient temperature of 12 °C) at the height of 1.50 m from the floor.

At 1.50 m from the floor, the velocity of the airflow profile for the winter case study is still higher than for the summer case study, but the difference is less critical than for 0.30 from the floor. The CFD model

also revealed that the furniture could impact the airflow path. Here, we noticed that the kitchen bench island seems to influence the kitchen extraction flow rate at 1.50 m, as the airflow path showed a higher velocity for the primary bathroom extraction.

In these CFD simulations, the difference in airflow velocities is only due to a temperature difference (inside - outside), as the wind velocity was selected at 0 $m.s^{-1}$ (reference case, Table 2). The difference between these two case studies will be exacerbated if we implement a wind velocity of 4.5 $m.s^{-1}$. The nodal network calculations (Table 2) showed a higher total airflow for the northern wind (winter) case study when compared to the southerly (summer) case study (124.8 $m^3.h^{-1}$ vs. 110.6 $m^3.h^{-1}$). An additional difference of 11.4 % airflow variation will be created with more pressure on the trickle vents (-7.9 Pa vs. + 19 Pa) if we implement a wind velocity of 4.5 $m.s^{-1}$.

This difference in airflow velocity could also impact the CO_2 concentration in the apartment.

3.2. Impact of the airflow on CO_2 concentration

This section investigates the ventilation efficiency in removing the CO_2 generated after four hours by the two adults in the living room and the child in the office. The CO_2 generation rate is constant for each occupant during sitting tasks/light activity, as displayed in Table 3. The wind velocity was set at 0 $m.s^{-1}$ (reference case, Table 2), and this simulation was undertaken with the internal doors open. We set the wind velocity to 0 $m.s^{-1}$ to remove the impact of the wind and focus only our investigation on the thermal effect.

Bhagat et al reported that the CO_2 distribution could be used as a proxy for virus particle distribution in the context of an infected occupant using the apartment as an isolation space [25].

Figs. 13 and 14 show the distribution of the CO_2 concentration (ppm) after four hours of occupancy in the summer (Fig. 13) and in the winter (Fig. 14) in the breathing zone (1.50 m from the floor).

The global Australian annual mean CO_2 concentration in 2021 was 414.4 ppm [48]. The CFD simulation software default set the outside CO_2 background level to 0 ppm. The values displayed in Figs. 13 and 14 must be increased by 414.4 ppm. As expected, the occupied rooms (the kitchen/living room with the two adults and the office with the child) show a higher level of CO_2 than the non-occupied room.

In the non-occupied rooms (primary bedroom, child's bedroom, and the child's bathroom), the CO_2 concentration (blue scale) is close to the outside level (414 ppm).

On average, Fig. 14 (winter case study) shows a lower CO_2 concentration in the kitchen/living room area, consistent with a higher airflow velocity reported in the winter (Fig. 12). In winter, the air seems better mixed in the apartment except for "CO_2 pockets" by the living room and office windows. The cold air trajectory is almost unidirectional downwards from the trickle ventilators (due to the temperature difference). The air flows at a high velocity close to the ground (0.3 m from the floor, Fig. 11) in the first metres from the windows (not well-mixed area) until it reaches the middle of the room, where the air warms up, and the mixing happens. At 1.5 m from the floor (Fig. 12), we again observed higher air velocities in the winter case than in the summer case (due to the kinetic energy gained at the entrance) and in the opposite direction to the flow at the ground level. In this configuration, these opposing currents form a pocket that could trap the CO_2.

For both cases, the results show a CO_2 level in the occupied rooms between 800 ppm and 1400 ppm after four-hour occupancy (the closer to the source of CO_2, i.e., occupants' location, the higher the CO_2 level). Table 4 shows the kitchen/living room and whole apartment mean CO_2 concentration obtained after four hours of occupancy. A lower mean CO_2 concentration for the winter case study was found compared to the summer case study (925 ppm vs. 1057 ppm in the kitchen/living room; 816 ppm vs. 850 ppm in the apartment).

The NCC performance requirement for suitable ventilation is set at 15 $L.s^{-1}$ extraction rate for a 90 m^2 two-bedroom apartment (with an air permeability rate of not more than 5 $m^3.hr^{-1}.m^{-2}$ at 50 Pa reference pressure) over four hours (NCC Part J1V4) [1]. Our case study used an extraction rate of 32.0 $L.s^{-1}$ (twice the NCC requirement). Despite setting an extraction rate twice the current rate level, the CO_2 level in the kitchen/living room area was estimated to be close to the 1000 ppm threshold for efficient ventilation in the Australian Indoor Air Quality Handbook [29,49].

Assuming a well-mixed air in the indoor compartment, the net change in CO_2 concentration in a room will be the result of the rate of CO_2 generation by occupants (activity, age, gender dependant), the CO_2 coming from outside, the CO_2 vented outside (extraction rate), and any chemical reaction removing CO_2.

The CO_2 is a good proxy for ventilation rate estimates and could also inform on the virus particle distribution in the breathing zone [25]. However, the CO_2 level should not be considered an overall indicator of the apartment's indoor air quality [49]. Persily (2022) reported, "*Indoor*

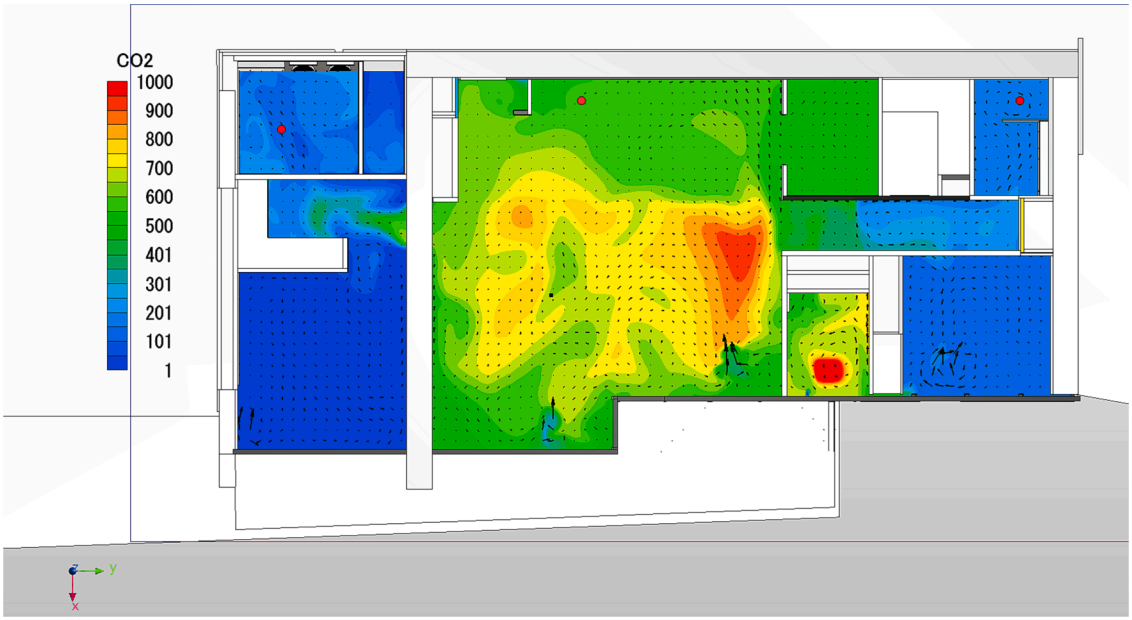

Fig. 13. CO_2 distribution after four hours of occupancy in the summer season (no wind) at 1.50 m from the floor (breathing zone).

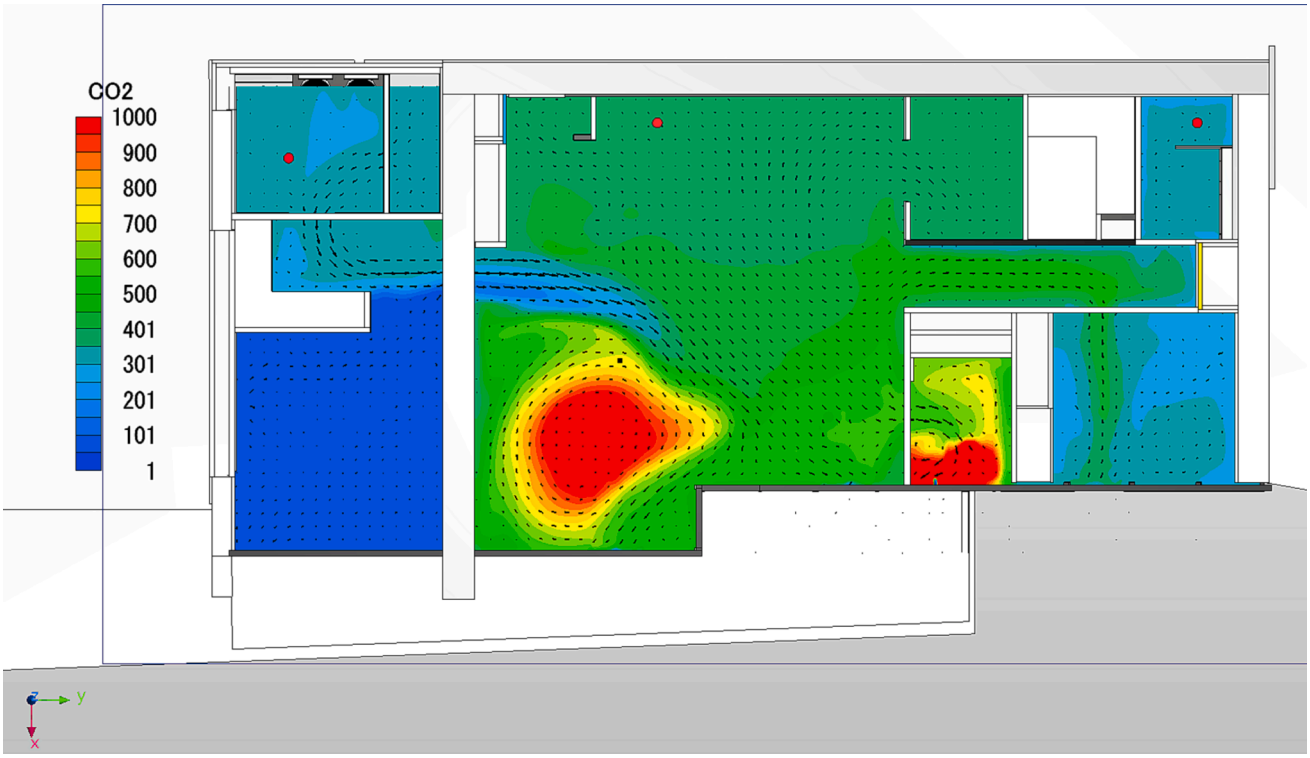

Fig. 14. CO_2 distribution after four hours of occupancy in the winter season (no wind) at 1.50 m from the floor (breathing zone).

Table 4
Mean CO_2 concentration in the kitchen/living room and the whole apartment after four hours.

Season	Wind	Intake temperature (°C)	Mean CO_2 in the kitchen/living room area (ppm)	Mean CO_2 in the whole apartment (ppm)
Summer	No wind	20	1057	850
Summer	4.5 m/s (South)	20	1065	845
Winter	No wind	12	925	816
Winter	4.5 m/s (North)	12	897	790

carbon dioxide (CO_2) concentrations have been considered for decades in evaluating indoor air quality (IAQ) and ventilation, and more recently in discussions of the risk of airborne infectious disease transmission. However, many of these applications reflect a lack of understanding of the connection between indoor CO_2 levels, ventilation, and IAQ" [50].

The common pollutants found in the indoor compartment are microorganisms, bio effluent, pollens, chemical gases (like VOC, nitrogen oxides, and carbon oxides), and inorganic contaminants such as metals, fibres, and particulate matter. CO_2, a carbon oxide, is only one of the listed common indoor pollutants and cannot be used as an overall indicator of indoor air quality. The concentration of other contaminants could also impact the Indoor Air Quality. Research shows evidence that poor ventilation (high CO_2 level) will impair the cognitive performance of building occupants; however, the level of impairment as a function of CO_2 concentration is not quantified yet [51].

3.3. Energy implications of the proposed strategy

We can identify two energy implications of the proposed strategy:

1) Adapted to the window frame, the trickle ventilators incorporate a passive wind dampener to manage draughts associated with high wind gusts and a shape memory alloy spring which will change the opening to external temperature (fully open above 18 °C and one-third open under 12 °C external temperature). For example, in winter, with an outside temperature of 12 °C, the incoming flow rate could be reduced from 115 $m^3.h^{-1}$ to 38 $m^3.h^{-1}$ (66 % decrease). The energy required to heat up these 38 m^3 of air from 12 °C to 20 °C equals 0.21 kWh each hour. When there could be a 66 % potential energy saving (0.43 kWh per hour) in winter due to the reduction of the effective open area of the trickle vent, there will be a reduction in the ventilation rate and potential impact on pollutant distribution and virus transmission.
2) Using trickle ventilators connected to extractor fans could contribute to night-time ventilative cooling type ventilation in summer (forcing the extraction flow). Following the calculations described in Tartarini et al. [52], we could estimate the daily cooling potential energy (QCCP) as:

$$QCCP = A \times H \times R \times \rho \times cp \times CCP = 13770 \text{ kJ (3.8kWh/day)}.$$

Where: A (net floor area) = 90 m^2, H (height of the ceiling) = 2.5 m, R (effective air change rate) = 0.51 h^{-1}, cp (specific heat capacity) = 1000 J. kg^{-1}. K^{-1}, ρ (air density) = 1.293 $kg.m^{-3}$, CCP (Climatic Cooling Potential for Melbourne daily mean in February) = 100 K.h (value extracted from [52]).

Our ventilation strategy could have good energy implications in summer (night-time ventilative cooling ventilation). However, in winter, our ventilation strategy has very limited energy implications. Reducing the effective trickle ventilator open area will negatively impact the ventilation rate and increase the risk of virus transmission.

4. Conclusions

The COVID-19 pandemic restrictions have forced many people to work from home. An appropriate ventilation rate is needed to provide occupants with a healthy environment. As occupants tend not to open windows, and mechanical ventilation (with heat recovery) is seldom installed in recently built environments, we need to inform about the

potential benefit of using trickle ventilators to assist occupants in ventilating their apartments.

Our project investigated a suitable ventilation solution (trickle ventilators connected to an extraction fan) in the context of doubling the current NCC performance requirement for continuous extraction in a Melbourne apartment occupied by two adults and a child over four hours.

The novelty of our work was to connect two approaches (the nodal network and the CFD) as the nodal network is less demanding regarding computational power than the CFD approach; the nodal network aimed to test a few combinations of input variables in a reduced time and then inform the CFD models.

The results showed that opening or closing the bedroom doors did not affect airflow. This means that the standard door undercut was sufficient to remove airflow resistance.

The findings show that the South wind on the North-facing building facade (input of the trickle ventilator) created a negative pressure, slightly decreasing the airflow. Furthermore, a non-protected extraction fan outlet could be impacted by a pressure of 18 Pa, creating a degraded regime and reducing the airflow by 13 %.

Our final apartment CFD model showed an impact of the input ambient air temperature, creating a cold air fall, which could create discomfort at about 30 cm from the floor. The results also showed that ambient cold air would contribute to a higher CO_2 concentration decrease but created small pockets of CO_2 that could increase the risk of virus transmission in the area where the pockets are created (if we assume that CO_2 and virus particles have similar distributions in the breathing zone). We doubled the current NCC performance requirement extraction rate. We found that occupants were still exposed to a CO_2 concentration of around 1000 ppm, which is considered to be the maximum level for adequate ventilation in the Australian Indoor Air Quality Handbook. If an occupant is infected, we recommend that all occupants wear a mask and respect social distancing. In addition, the extraction rate should be increased as our results showed that 10.0 $L.s^{-1}$ per person is insufficient for effective ventilation.

CFD is an excellent tool for investigating the airflow velocity and the ventilation efficiency to remove the CO_2 generated by occupants. The CO_2 concentration in the different rooms indicated the capacity of the ventilation system to extract CO_2. We can only assume that some other contaminants will follow the same path, but this is only an assumption. The CO_2 metric can evaluate the ventilation rates relative to a design value. Still, without a complete understanding of the significance of the other potential contaminants, we cannot conclude about the indoor air quality in this apartment.

Biler [53] reported a lack of comprehensive CFD studies involving trickle ventilators coupled to extraction fans under a continuous flow rate. Our study contributed to inform this research area; however, it consists of only one case study. Further case studies will be investigated in detail before making general recommendations. We also plan to deploy a monitoring platform in the studied apartment to validate our findings (at the time of the writing, the studied apartment was not constructed).

CRediT authorship contribution statement

Mikael Boulic: . **Pierre Bombardier:** Conceptualization, Methodology, Software, Writing – original draft, Writing – review & editing. **Zain Zaidi:** Methodology, Software, Writing – review & editing. **Andrew Russell:** Writing – review & editing. **David Waters:** Conceptualization, Resources, Writing – review & editing. **Andries van Heerden:** Writing – review & editing.

Declaration of competing interest

The authors declare that they have no known competing financial interests or personal relationships that could have appeared to influence the work reported in this paper.

Data availability

Data will be made available on request.

References

[1] ABCB., (2023). NCC 2022 - Volume 1, for Class 2 to 9 buildings (commercial, industrial, and multi-residential buildings), the Australian Building Codes Board, Canberra, Australia.

[2] M. Ambrose, M. James, A. Law, P. Osman, S. White, The evaluation of 5-Star energy efficiency standard for residential buildings – Final Report, Department of Industry, Canberra, 2013, p. 2013.

[3] M. Ambrose, M. Syme, Airtightness of new australian residential buildings, Procedia Eng. 180 (2017) 1877–7058, https://doi.org/10.1016/j.proeng.2017.04.162. ISSN 33–40.

[4] G. Overton, S. McNeil, Airtightness of selected apartments in New Zealand, BRANZ Ltd., Judgeford, New Zealand, 2020. BRANZ Study Report SR455.

[5] McNeil, S., Plagmann, M., McDowall, P., Bassett, M., (2015). The role of ventilation in managing moisture inside New Zealand homes. BRANZ Study Report SR341. Judgeford, New Zealand: BRANZ Ltd.

[6] M. Dewsbury, T. Law, J. Potgieter, D. Fitz-Gerald, B. McComish, T. Chandler, A. Soudan, Scoping study of condensation in residential buildings - Final report, University of Tasmania, Hobart, Australia, Australian Building Codes Board; Department of Industry Innovation and Science, 2016.

[7] J. Berneiser, S. Auerswald, D. Maier, S. Gölz, N. Carbonare, T. Pflug, Feeling the breeze? Ventilation practices and occupant requirements for mechanical ventilation in residential buildings, Energy and Buildings, ISSN 113702 (2023) 0378–7788, https://doi.org/10.1016/j.enbuild.2023.113702.

[8] De Gids, W., Borsboom, W.Z., (2023). TN 72: Ventilation requirements and rationale behind. Standards and Regulations of dwellings, office rooms and classrooms. 56 pp, AIVC Technical Note 72. The Air Infiltration and Ventilation Centre (AIVC), Ghent, Belgium.

[9] G. Correiax, L. Rodrigues, M. Gameiro da Silva, T. Gonçalves, Airborne route and bad use of ventilation systems as non-negligible factors in SARS-CoV-2 transmission, Med Hypotheses. 141 (2020), 109781, https://doi.org/10.1016/j.mehy.2020.109781.

[10] H. Dai, B. Zhao, Association of the infection probability of COVID-19 with ventilation rates in confined spaces, Build Simul. 13 (6) (2020) 1321–1327, https://doi.org/10.1007/s12273-020-0703-5.

[11] E. Lepore, P. Aguilera Benito, C. Piña Ramírez, G. Viccione, Indoors ventilation in times of confinement by SARS-CoV-2 epidemic: A comparative approach between Spain and Italy, Sustain. Cities Soc. 72 (2021) 2210–6707, https://doi.org/10.1016/j.scs.2021.103051.

[12] L. Morawska, J.W. Tang, W. Bahnfleth, P.M. Bluyssen, A. Boerstra, G. Buonanno, J. Cao, S. Dancer, A. Floto, F. Franchimon, C. Haworth, J. Hogeling, C. Isaxon, J. L. Jimenez, J. Kurnitski, Y. Li, M. Loomans, G. Marks, L.C. Marr, L. Mazzarella, M. Yao, How can airborne transmission of COVID-19 indoors be minimised? Environ. Int. 142 (2020), 105832 https://doi.org/10.1016/j.envint.2020.105832.

[13] World Health Organization, Roadmap to improve and ensure good indoor ventilation in the context of COVID-19, World Health Organization, Geneva PP - Geneva, 2021.

[14] C.F. Picard, C.R. Salis, L., Abadie, M.,, Home quarantine: A numerical evaluation of SARS-CoV-2 spread in a single-family house, Indoor Air 32 (2022), e13035, https://doi.org/10.1111/ina.13035.

[15] G. Guyot, S. Sayah, S. Guernouti, A. Mélois, Role of ventilation on the transmission of viruses in buildings, from a single zone to a multizone approach, Indoor Air 32 (8) (2022), e13097, https://doi.org/10.1111/ina.13097.

[16] F. Jara-Baeza, P. Rajagopalan, M. Andamon, A holistic assessment of indoor environmental quality perception in Australian high-rise social housing, Energ. Buildings 284 (2023) 0378–7788, https://doi.org/10.1016/j.enbuild.2023.112859.

[17] M.A. Navas-Martín, T. Cuerdo-Vilches, Natural ventilation as a healthy habit during the first wave of the COVID-19 pandemic: an analysis of the frequency of window opening in Spanish homes, J. Build. Eng. 65 (2023) 2352–7102, https://doi.org/10.1016/j.jobe.2022.105649.

[18] F. Xu, Z. Gao, Study on indoor air quality and fresh air energy consumption under different ventilation modes in 24-hour occupied bedrooms in Nanjing, using Modelica-based simulation, Energ. Build. 257 (2022) 0378–7788, https://doi.org/10.1016/j.enbuild.2021.111805.

[19] C.I.B.S.E. Application Manual, Am 11, Building Performance Modelling, Chartered Institute of Building Services Engineers, London, 2015.

[20] H.K. Versteeg, W. Malalasekera, An Introduction to Computational Fluid Dynamics: the Finite, volume method, Pearson Education Ltd, Harlow, Essex, England, 2007.

[21] R. Guichard, Simulation of the unsteady dispersion of asbestos fibres from a containment zone due to wind effects using a coupled CFD-network approach. 10Th International Conference on Multiphase Flow, ICMF 2019, Rio De Janeiro, 2019.

[22] J.A. Clarke, J.L.M. Hensen, C.O.R. Negrao, Predicting indoor airflow by combining network approach, CFD and thermal simulation. Implementing the results of ventilation research, 1995.

[23] S. Kato, W. Zhang, A review: coupled simulation of CFD and network model for heat and contaminant transport in a building, J. Asian Architec. Build. Eng. 13 (1) (2014) 231–238, https://doi.org/10.3130/jaabe.13.231.
[24] F. Zhao, S.L. Zou, S.L. Xu, X. Wang, J.L. Wang, D.W. Tang, A novel approach for radionuclide diffusion in the enclosed environment of a marine nuclear reactor during a severe accident, Nucl. Sci. Tech. 33 (2022) 19, https://doi.org/10.1007/s41365-022-01007-z.
[25] R.K. Bhagat, M.D. Wykes, S.B. Dalziel, P. Linden, Effects of ventilation on the indoor spread of COVID-19, J. Fluid Mech. 903 (2020) F1, https://doi.org/10.1017/jfm.2020.720.
[26] Bruce Henderson Architects (2018). https://www.bh-architects.com/urban-growth-and-apartment-sizes-in-melbourne, accessed on 27th September 2023.
[27] Zhou, C., (2017). https://www.domain.com.au/news/melbourne-apartments-number-of-bedrooms-hard-to-pinpoint-as-developers-reign-20170203-gu35rn/, accessed on 27th September 2023.
[28] Ventient model SCW-SH700, https://proctorgroup.com.au/ventient/ventient-scw-sh/ accessed on 29th June 2023.
[29] NCC IAQVM Handbook., (2023). The National Construction Code Indoor Air Quality Verification Methods Handbook. The Australian Building Codes Board, Canberra, Australia. https://ncc.abcb.gov.au/sites/default/files/resources/2023/Handbook-Indoor-Air-Quality-Verification-Methods-NCC-2022.pdf.
[30] Holmes, J.D., (2021). Wind climate of the Melbourne metropolitan area. Proceedings of the Royal Society of Victoria 133, 82-92. doi: 10.1071/RS21011.
[31] Wind data from Melbourne Essendon Field Airport Weather Station (WeatherSpark, 2023). https://weatherspark.com/y/144227/Average-Weather-in-Melbourne-Australia-Year-Round# accessed on 29th June 2023.
[32] Z. Stevanovic, D. Mumovic, M. Kavgic, Indoor Air Quality and Ventilation Modelling, in: D. Mumovic, M. Santamouris (Eds.), A Handbook of Sustainable Building Design and Engineering: an Integrated Approach to Energy, Health and Operational Performance, (1st ed.)., Routledge, 2009.
[33] V. Yakhot, S.A. Orszag, Renormalisation group analysis of turbulence. I. Basic theory, J. Sci. Comput. 1 (1986) 3–51.
[34] J. Lu, S. Zhu, M.K. Kim, J. Srebric, A review of CFD analysis methods for personalised ventilation (PV). Indoor Built Environments, Sustainability 11 (2019) 4166.
[35] Gupta, D., and Khare, V.R., (2021). Natural Ventilation Design: Predicted and Measured Performance of a Hostel Building in Composite Climate of India, Energy and Built Environment, Volume 2, Issue 1, Pages 82-93, ISSN 2666-1233, doi: 10.1016/j.enbenv.2020.06.003.
[36] K. Abe, T. Kondoh, Y. Nagano, A new turbulence model for predicting fluid flow and heat transfer in separating and reattaching flows - I. flow field calculations, Int. J. Heat Mass Transfer 37 (1994) 139–151.
[37] scSTREAM.,, User's Guide Basics of CFD Analysis: Linear low-Reynolds number turbulence model section, Cradle CFD scSTREAM, Hexagon AB, Stockholm, Sweden, 2023.
[38] Hassan, Y., (2017). An overview of computational fluid dynamics and nuclear applications, in Francesco D'Auria (Eds), Thermal hydraulics of water-cooled nuclear reactors, Woodhead Publishing, Pages 729-829, ISBN 9780081006627.
[39] D.N. Sørensen, P.V. Nielsen, Quality control of computational fluid dynamics in indoor Environments, Indoor Air 13 (2003) 2–17.
[40] J. Franke, A. Hellsten, K.H. Schlünzen, B. Carissimo, The COST 732 Best practice guideline for the CFD simulation of flows in the urban environment - a summary, Int. J. Environ. Pollut. 44 (1–4) (2011) 419–427.
[41] scSTREAM V13 CRADLE CFD., (2017). Introductory Seminar No. 1 https://www.cradle-cfd.com/dcms_media/other/webinar_scSTREAM_101_V13.pdf accessed on 29th June 2023.
[42] N. Le Roux, X. Faure, C. Inard, S. Soares, L. Ricciardi, Reduced-scale study of transient flows inside mechanically ventilated buildings subjected to wind and internal overpressure effects, Build. Environ. 62 (2013) 18–32, https://doi.org/10.1016/j.buildenv.2013.01.011.
[43] T. Le Dez, J. Richard, C. Inard, N. Le Roux, F. Demouge, X. Faure, L. Ricciardi, Reduced-scale study of the coupling between thermal and wind effects on the ventilation systems of nuclear facilities, Int. J. Vent. 20 (1) (2021) 1–19, https://doi.org/10.1080/14733315.2019.1693135.
[44] W. Plumecocq, L. Audouin, J.P. Joret, H. Pretrel, Numerical method for determining water droplets size distributions of spray nozzles using a two-zone model, Nucl. Eng. Des. 324 (2017) 67–77.
[45] E. Chojnacki, W. Plumecocq, L. Audouin, An expert system based on a Bayesian network for fire safety analysis in nuclear area, Fire Saf. J. 105 (2019) 28–40, https://doi.org/10.1016/j.firesaf.2019.02.007.
[46] Irsn.,, User guide of the SYLVIA V11 software, Institut de Radioprotection et de Sureté Nucléaire, Fontenay aux Roses, France, 2019.
[47] A. Persily, L. de Jonge, Carbon dioxide generation rates for building occupants, Indoor Air 27 (5) (2017) 868–879.
[48] Australian Government Bureau of Meteorology, State of the Climate 2022 http://www.bom.gov.au/state-of-the-climate/greenhouse-gas-levels.shtml.
[49] Persily, A., (2020). Quit blaming ASHRAE Standard 62.1 for 1000 ppm CO_2, The 16th Conference of the International Society of Indoor Air Quality & Climate (Indoor Air 2020), Seoul, KR, [online], https://tsapps.nist.gov/publication/get_pdf.cfm?pub_id=929997 accessed on 29th June 2023.
[50] A. Persily, Development and application of an indoor carbon dioxide metric, Indoor Air 32 (2022) e13059.
[51] B. Du, M.C. Tandoc, M.L. Mack, J.A. Siegel, Indoor CO_2 concentrations and cognitive function: a critical review, Indoor Air 30 (2020) 1067–1082, https://doi.org/10.1111/ina.12706.
[52] F. Tartarini, M. Fiorentini, L. Ledo Gomis, P. Cooper, in: Ventilative cooling potential of buildings in Australia, IOP Conference Series: Materials Science and Engineering, 2019, https://doi.org/10.1088/1757-899X/609/3/032052.
[53] A. Biler, A. Unlu Tavil, Y. Su, N. Khan, A review of performance specifications and studies of trickle vents, Buildings 8 (2018) 152, https://doi.org/10.3390/buildings8110152.